Published in *Computer Simulation Studies in Condensed-Matter Physics XII*, p. 86–99, edited by D.P. Landau, S.P. Lewis and H.B. Schüttler (Springer, Heidelberg, 2000).

Monte Carlo Simulation of Spin Models with Long-Range Interactions

Erik Luijten

Max-Planck-Institut für Polymerforschung, D-55021 Mainz, Germany
Institut für Physik, Johannes Gutenberg-Universität, D-55099 Mainz, Germany

Abstract. An efficient Monte Carlo algorithm for the simulation of spin models with long-range interactions is discussed. Its central feature is that the number of operations required to flip a spin is independent of the number of interactions between this spin and the other spins in the system. In addition, critical slowing down is strongly suppressed. In order to illustrate the range of applicability of the algorithm, two specific examples are presented. First, some aspects of the Kosterlitz–Thouless transition in the one-dimensional Ising chain with inverse-square interactions are calculated. Secondly, the crossover from Ising-like to classical critical behavior in two-dimensional systems is studied for several different interaction profiles.

1 Introduction

For a long time, systems with long-range interactions have posed a great challenge to the application of Monte Carlo (MC) methods. Due to the large number of interactions that have to be taken into account, simulations are very time consuming and hence restricted to relatively small system sizes. Alternatively, the interaction is truncated beyond a certain distance, which may introduce severe errors in the calculation. Thus, it is desirable to have an algorithm at one's disposal that allows the efficient simulation of systems with long-range interactions without making any approximation except for the inherent statistical errors. A few years ago, an algorithm fulfilling these requirements was indeed introduced for the simulation of spin models [1]. It is based on the cluster method introduced by Swendsen and Wang [2] and has the crucial property that the number of operations required to add a single spin to a cluster is *independent* of the number of interactions of this spin with other spins in the system. Thus, the numerical effort to simulate ferromagnetic long-range models becomes comparable to that for short-range models. Close to the critical point the application of the algorithm becomes particularly profitable, since there one also benefits from the inherent reduction in critical slowing down in cluster algorithms. It is the purpose of the present paper to discuss this algorithm in some more detail and to illustrate its power by means of some selected applications.

2 Description of the Algorithm

2.1 Conventional Wolff Cluster Algorithm

To set the stage, we first briefly discuss the standard cluster algorithm for a system with short-range interactions. For simplicity, we will employ a formulation in terms of the Wolff cluster algorithm [3] rather than that of Swendsen and Wang (SW). It should be noted, however, that the modifications required for the simulation of long-range interactions pertain to the cluster-formation process only, and hence can equally well be combined with the SW variant. Since a detailed derivation of the Wolff algorithm can be found in numerous references, we restrict ourselves here to a schematic outline. Consider a d-dimensional lattice structure, where on each lattice site i a spin s_i is placed, which can take the values ± 1 and which has a ferromagnetic coupling K with its nearest neighbors. Thus, the system is described by the following Hamiltonian,

$$\beta\mathcal{H} = -K \sum_{i<j} s_i s_j \ , \tag{1}$$

where the sum runs over all pairs of nearest neighbors. At each Monte Carlo step, a cluster of spins with identical sign is flipped. The nonlocal character of this operation leads to a rapid decay of correlations. The crucial step is the identification of a cluster:

1. Randomly choose a spin s_i from the lattice.
2. Consider each spin that interacts with spin s_i. It is added to the cluster with a probability $p = 1 - \exp(-2K)$, provided that it has the same sign as s_i.
3. Repeat step 2 in turn for each spin that is newly added to the cluster, where one now considers all spins that interact with this spin, rather than with s_i. This is iterated until all neighbors of all spins in the cluster have been considered for inclusion.

This cluster-building process is based on the Kasteleyn–Fortuin mapping [4,5] of the Potts model on a bond-percolation model. This mapping allows a generalization of the outlined procedure to systems with different interaction strengths K_j. In the second step, a spin is simply added with a probability $p_j = 1 - \exp(-2K_j)$ if the interaction strength with the spin s_i is equal to K_j. As a side note, it is remarked that this implies that a cluster now not necessarily can be visualized as a contiguous collection of spins.

Although one can thus easily devise a cluster algorithm for systems with long-range interactions, its efficiency rapidly decreases with an increasing number of interactions. Indeed, the typical value for the coupling K in such a system will be relatively small and hence each single spin that is considered for inclusion in the cluster will be added only with a small probability. So, a lot of operations are required to add a single spin to the cluster.

2.2 Efficient Construction of Clusters

In order to illustrate our approach, we take the example of a one-dimensional chain with a spin–spin interaction that decays as a power-law, $K_{ij} = f r_{ij}^{-1-\sigma}$. The cluster-building process starts with a spin on a randomly chosen site i and all other spins in the system are added to the cluster with a probability $p(s_i, s_j) = \delta_{s_i s_j} p_{ij}$, where $p_{ij} = 1 - \exp[-2f|i-j|^{-(1+\sigma)}]$. For each spin that is actually added to the cluster, its address is also placed on the *stack*. When all spins interacting with the first one have been considered, we read a new spin from the stack and repeat the process, until the stack is empty. The spin from which we are currently adding spins will be called the *current spin*. In order to avoid considering each single spin for inclusion in the cluster, we split up the probability $p(s_i, s_j)$ into two parts, namely the Kronecker delta testing whether the spins s_i and s_j have the same sign and the "provisional" probability p_{ij}. This enables us to define the concept of the *cumulative probability* $C(j)$, from which we can read off which spin is the next one to be provisionally added to the cluster,

$$C(j) \equiv \sum_{n=1}^{j} P(n) \tag{2}$$

with

$$P(n) = \left[\prod_{m=1}^{n-1} (1 - p_m) \right] p_n \ . \tag{3}$$

$p_j \equiv 1 - \exp(-2K_j)$ is an abbreviation for p_{0j} (and $K_j \equiv K_{0j}$), i.e., we define the origin at the position of the current spin. $P(n)$ is the probability that in the first step $n-1$ spins are skipped and the nth spin is provisionally added. Now the next spin j that is provisionally added is determined by a (pseudo)random number $g \in [0, 1\rangle$: $j-1$ spins are skipped if $C(j-1) \leq g < C(j)$. If the jth spin has indeed the same sign as the current spin then s_j is added to the cluster. Subsequently we skip again a number of spins before another spin at a distance $k > j$ is provisionally added. Due to the requirement $k > j$ we must shift the function P,

$$P_j(k) = \left[\prod_{m=j+1}^{k-1} (1 - p_m) \right] p_k \ , \tag{4}$$

and Eq. (3) is simply a special case of Eq. (4). The appropriate cumulative probability is now given by a generalization of Eq. (2),

$$C_j(k) = \sum_{n=j+1}^{k} P_j(n) \ . \tag{5}$$

By using the specific form of the probability p_{ij} one finds that this reduces to

$$C_j(k) = 1 - \exp\left(-2 \sum_{n=j+1}^{k} K_n\right) , \tag{6}$$

i.e., the probability that the next spin that will be added lies at a distance in the range $[j+1, k]$ is given by an expression that has the same form as the original probability, in which the coupling constant is replaced by the sum of all the couplings with the spins in this range.

We now consider two possibilities of calculating the distance k from a given $C_j(k)$. A straightforward approach is the construction of a look-up table. This means that we explicitly carry out the sum in (6) for a large number of distances k, up to a certain cutoff M, and store the results in a table. Then, after drawing a random number, we can derive the corresponding spin distance from this table. In principle we need for each value of j another look-up table containing the $C_j(k)$. This is hardly feasible and fortunately not necessary, as follows from a comparison of Eqs. (2) and (5). Namely (assume $k > j$),

$$\begin{aligned} C(k) \;=\; C_0(k) &= C(j) + \left[\prod_{i=1}^{j}(1-p_i)\right] C_j(k) \\ &= C(j) + [1 - C(j)]\, C_j(k) \end{aligned} \tag{7}$$

or $C_j(k) = [C(k) - C(j)]/[1 - C(j)]$. So we can calculate $C_j(k)$ directly from $C(k)$. In practice one realizes this by using the distance j of the previous spin that was provisionally added to rescale the (new) random number g to $g' \in [C(j), 1\rangle$; $g' = C(j) + [1 - C(j)]g$. Since we only consider ferromagnetic interactions, $\lim_{j\to\infty} C(j)$ exists and is smaller than 1, cf. Eq. (6).

This method is very fast, since we have to calculate all cumulative probabilities only once, but it has two major drawbacks. First, we can accommodate only a limited number of spin distances in our look-up table and must therefore devise some approximation scheme to handle the tail of the long-range interaction, which is essential for the critical behavior in the case of slowly decaying interactions (small σ). This issue is addressed below. Secondly, this method is impractical in more than one dimension, as the number of distances for which the cumulative probability has to be calculated rapidly increases with the dimensionality of the system (for a fixed cutoff).

For interactions that can be explicitly summed there exists a powerful alternative. In those cases, Eq. (6) can be solved for k, yielding an expression for the spin distance in terms of $C_j(k)$, i.e., in terms of the random number g. Especially for the study of critical phenomena this is often a feasible approach, since in many cases one can modify an interaction such it can be explicitly integrated by only adding irrelevant terms that do not affect the universal critical properties. As an example, we consider again the power-law

interaction $K_{ij} = f|i-j|^{-(1+\sigma)}$. The corresponding sum appearing in the right-hand side of (6) is (for $j = 0$) the truncated Riemann zeta function, which cannot be expressed in closed form. However, upon approximation of this sum by the integral

$$\sum_{n=j}^{k} K_n = \sum_{n=j}^{k} \frac{f}{n^{1+\sigma}} \approx f \int_{j-\frac{1}{2}}^{k+\frac{1}{2}} dx\, x^{-(1+\sigma)} \tag{8}$$

one still has an exact Monte Carlo scheme, but for an interaction

$$K(|i-j|) = f \int_{|i-j|-\frac{1}{2}}^{|i-j|+\frac{1}{2}} dx\, x^{-(1+\sigma)} \; . \tag{9}$$

Both interactions belong to the same universality class, so that, e.g., for the determination of critical exponents one is free to make the most convenient choice. Of course, all nonuniversal quantities, such as the critical temperature, will have different values. For the modified interaction, Eq. (6) reduces to

$$C_j(k) = 1 - \exp\left[-\frac{2f}{\sigma}\left(\frac{1}{j^\sigma} - \frac{1}{k^\sigma}\right)\right] \; , \tag{10}$$

where it should be noted that this is only the probability for adding a spin that lies in a single direction. We have not written $j + \frac{1}{2}$ and $k + \frac{1}{2}$ instead of j and k, because we prefer to use continuous coordinates, which only in the last stage are rounded to a lattice site. Equating $C_j(k)$ to the random number g we find

$$k = \left[j^{-\sigma} + \frac{\sigma}{2f}\ln(1-g)\right]^{-1/\sigma} \; . \tag{11}$$

Rescaling of the random number is no longer required: the lowest value, $g = 0$, leads to a provisionally added spin at the same distance as the previous one, $k = j$. If $g = C_j(\infty) = 1-\exp[-(2f/\sigma)j^{-\sigma}]$ the next provisionally added spin lies at infinity and thus $g \in [C_j(\infty), 1\rangle$ yields no spin at all. Once the coordinates of the next provisionally added spin have been calculated by rounding to the nearest integer coordinate, the periodic boundary conditions are applied to map this coordinate onto a lattice site. For the following provisionally added spin, j is set equal to k (*not* to the rounded distance!) and a new k is determined. If no spin has been added yet, j is set to $\frac{1}{2}$, the lowest possible distance. For higher dimensionalities, $d-1$ additional random numbers are required to determine the direction in which the next spin is added.

The above-mentioned limited size M of the look-up table can now be coped with as well: beyond the spin distance M the sum in (6) is approximated by an integral. Thus, if the random number g lies in the interval $[C(M), C(\infty)\rangle$, the spin distance k is determined from a modified version of (11), where the lower part of the integral is replaced by an explicit sum

$$k = \left[\left(M+\frac{1}{2}\right)^{-\sigma} + \sigma\left(\frac{1}{2f}\ln(1-g) + \sum_{n=1}^{M}\frac{1}{n^{1+\sigma}}\right)\right]^{-1/\sigma} \; . \tag{12}$$

2.3 Discussion

Finally, we briefly illustrate the efficiency of the algorithm by means of an example. If the probability p were equal for each spin pair, one out of p^{-1} spins would be added to the cluster, and it would take $\mathcal{O}(p^{-1}) \sim \mathcal{O}(L^0)$ operations per spin to update a configuration, compared to $\mathcal{O}(L^d)$ operations *per spin* for a Metropolis algorithm. Taking into account the decrease in critical slowing down, we see that the efficiency of this method is typically a factor $\mathcal{O}(L^{d+z})$ larger than the conventional Monte Carlo algorithm. In the case of a large but finite interaction range R, such as for the two-dimensional equivalent-neighbor model discussed in Sec. 3.2, one gains a factor $\mathcal{O}(R^d L^z)$, provided that critical slowing down is completely suppressed in the cluster algorithm. Far from the critical temperature, the factor L^z disappears, but one still has the advantage of a speed increase proportional to the number of interactions per spin.

3 Applications

3.1 The Inverse-Square Ising Chain

As a first application, we consider the Ising chain introduced before, with spin–spin interactions that decay as $f r_{ij}^{-1-\sigma}$. Unlike the Ising chain with short-range interactions, in which no long-range order is possible for nonzero temperatures, this system exhibits a remarkably rich behavior. The interested reader is referred to Ref. [6] for a review. In summary, the system exhibits mean-field-like critical behavior for $0 < \sigma \leq \frac{1}{2}$ and nonclassical critical behavior for $\frac{1}{2} < \sigma < 1$, with critical exponents that depend on σ. For $\sigma > 1$ the interactions are essentially short-ranged. At $\sigma = 1$, the so-called inverse-square Ising model, we have a very interesting situation: the spin chain displays a phase transition which is the one-dimensional analog of the Kosterlitz–Thouless (KT) transition in the two-dimensional XY model. It has close connections to a variety of physical applications, such as the Kondo problem, quantum tunneling in a two-state system coupled to a dissipative environment, quark confinement, etc. Although the KT transition has received an enormous amount of attention over the past decades, there are still open questions. Two peculiar properties of this transition are: (1) at the critical temperature T_c the order parameter exhibits a singular behavior *superposed* on a jump like one finds for a first-order transition; (2) the correlation length ξ and the susceptibility χ diverge exponentially for $T \downarrow T_\mathrm{c}$: $\xi = \xi_0 \exp[B_\xi/(T - T_\mathrm{c})^\nu]$ and $\chi = \chi_0 \exp[B_\chi/(T - T_\mathrm{c})^\nu]$, with $\nu = \frac{1}{2}$. These and related critical properties turn out to be very difficult to verify in numerical simulations of two-dimensional models, because the finite-size effects decay only logarithmically. The one-dimensional model, which now can be simulated with comparable efficiency, clearly offers a great advantage: rather than a linear system size of $\mathcal{O}(10^3)$, like for $d = 2$, one can reach system sizes

$L = \mathcal{O}(10^6)$ and thus approach the critical point much closer. Since a detailed description of the critical properties and their numerical determination is beyond the scope of this paper, we restrict ourselves here to a study of the quantity $\Psi \equiv Km^2$, where K is the coupling constant and m the magnetization density, and its application for the determination of T_c (or, equivalently, its inverse, the critical coupling K_c). It can be shown that Ψ is the analog of the spin-wave stiffness in the 2D XY model. Just like the latter quantity is predicted to have a universal jump $2/\pi$ at criticality, Ψ is expected to have a jump of size $\frac{1}{2}$ [7]. Indeed, in Figure 1, where $\Psi(K, L)$ is shown for system sizes up to $L = 400\,000$, one can already clearly observe how such a jump develops with increasing system size. The superposed square-root singularity,

$$\Psi(K, \infty) = \Psi(K_\mathrm{c}, \infty) + C\sqrt{K - K_\mathrm{c}} + \mathcal{O}(K - K_\mathrm{c}) \,, \tag{13}$$

is shown in the inset.

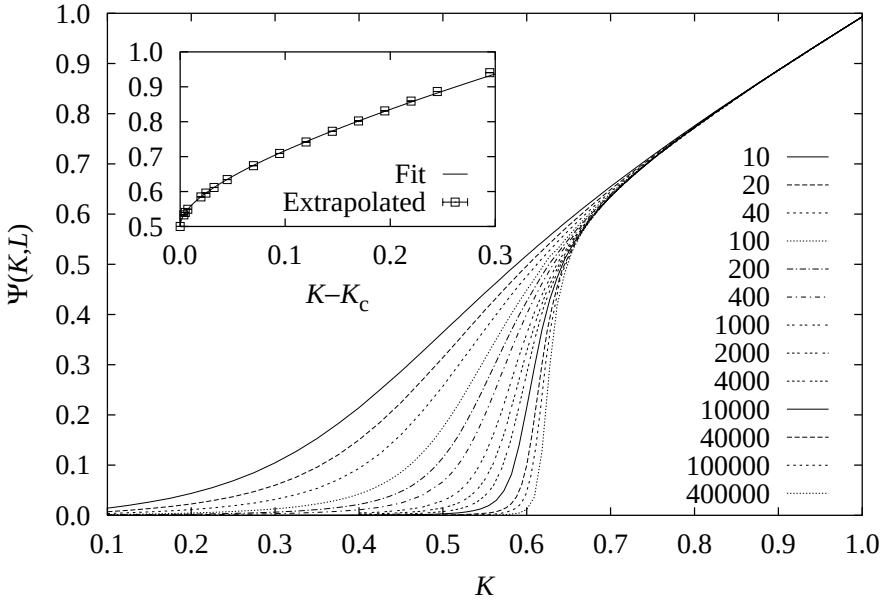

Fig. 1. The quantity $\Psi = Km^2$ as a function of the coupling K, for system sizes $10 \le L \le 400\,000$. The inset shows $\lim_{L\to\infty} \Psi(K, L)$ for $K > K_\mathrm{c}$.

We consider now three distinct ways to use this quantity for the determination of K_c, which for phase transitions in this universality class is notoriously difficult. First, one may use the predicted singular behavior of Ψ for $K > K_\mathrm{c}$. To this end, the finite-size data at fixed couplings first must be

extrapolated to the thermodynamic limit. By integrating the RG equations one finds [7] that $\Psi(K,L)$ obeys a finite-size expansion of the form

$$\Psi(K,L) = \Psi(K,\infty)\left\{1 + a_1 L^{-2[\bar{\Psi}-1]} + a_2 L^{-4[\bar{\Psi}-1]} + \cdots\right\} , \tag{14}$$

where $\bar{\Psi} = \Psi(K,\infty)/\Psi(K_\mathrm{c},\infty)$ and the ellipsis denotes higher-order terms. The resulting estimates for $\Psi(K,\infty)$ are then fitted to Eq. (13), in which $\Psi(K_\mathrm{c},L)$ is kept fixed at $\frac{1}{2}$. This yielded $K_\mathrm{c} = 0.6552\ (2)$. Secondly, $\Psi(K,L)$ in the high-temperature regime $K < K_\mathrm{c}$ may be used to estimate K_c. Indeed, within the finite-size regime one expects two types of corrections to scaling: corrections due to irrelevant fields, which decay as powers of $1/\ln L$, and temperature-dependent corrections which can be expanded in terms of L/ξ. A least-squares fit of the numerical data to an expansion of the form

$$\Psi(K,L) = \Psi(K_\mathrm{c},\infty) + a_1\frac{L}{\xi} + a_2\left(\frac{L}{\xi}\right)^2 + \cdots + \frac{b_1}{\ln L} + \frac{b_2}{(\ln L)^2} + \cdots \tag{15}$$

has yielded $\Psi(K_\mathrm{c},\infty) = 0.496\ (3)$ and $K_\mathrm{c} = 0.6548\ (14)$. Fixing $\Psi(K_\mathrm{c},\infty)$ at the predicted value $\frac{1}{2}$ we found $K_\mathrm{c} = 0.6555\ (4)$. Finally, a very straightforward but remarkably effective approach is to fit a set of finite-size data for $\Psi(K,L)$ at *fixed* coupling to an expression of the form of Eq. (15), in which all temperature-dependent terms have been omitted, i.e., one *assumes* that $K = K_\mathrm{c}$. Although in principle such a fit should only work at the true critical coupling, it turns out that least-squares fits of a good quality can be obtained over a range of couplings. However, the resulting estimate of $\Psi(K,\infty)$ is a monotonously increasing function of K and K_c can be determined from the requirement that $\Psi(K_\mathrm{c},\infty) = \frac{1}{2}$, yielding $K_\mathrm{c} = 0.65515\ (20)$.

Table 1. Some estimates (in chronological order) for the critical coupling K_c of the inverse-square Ising chain.

Reference	K_c	Method
[8]	≈ 0.612	Exact summation + Padé approximants
[9]	≈ 0.635	RG
[10]	≈ 0.490	Extended mean-field approach
[11]	0.657 (3)	Series expansion
[12]	≥ 0.441	Extended mean-field approach
[13]	$\geq \frac{1}{2}$	Analytical
[14]	≈ 0.562	Coherent-anomaly method
[15]	0.5	Variational method
[16]	0.590 (5)	Cycle expansion
[17]	0.615	Transfer matrix
[18]	≥ 0.61128	Extended mean-field approach
[19]	$6/\pi^2 \approx 0.6079$	RG (conjectured to be exact)
This work	0.6552 (2)	MC

It is rewarding that the three different methods yield consistent estimates for the critical coupling. Table 1 summarizes several estimates for K_c, obtained by a variety of methods. Remarkably, most numerical results (of which only few carry an explicit estimate of the uncertainty) suggest a critical coupling around 0.61. Our estimate lies considerably higher and only agrees with the series-expansion result of Ref. [11]. All methods that rely on an extension of mean-field theory clearly suffer from the extremely slow convergence to the thermodynamic limit. The exact conjecture of Ref. [19] (which is, interestingly, precisely twice as large as the mean-field result $3/\pi^2$) has been refuted.

3.2 Crossover from Ising-Like to Classical Critical Behavior

In order to illustrate that also for interactions with a large but strictly finite range the presented algorithm offers great advantages, we consider the so-called "equivalent-neighbor" model. This is a simple generalization of the Ising model, in which each spin interacts equally strongly with all its neighbors within a distance R_m. In the limit $R_m \to \infty$ this model becomes equivalent to the exactly-solved mean-field model, whereas all systems with a *finite* interaction range belong to the Ising universality class. Since an exact solution for the latter case is lacking for $d = 3$, it is interesting to study the variation of critical properties as a function of R_m (cf. Ref. [20]). Another, experimentally very relevant, application of this model will be discussed here. As is well known, many thermodynamic properties show a characteristic power-law divergence upon approach of a critical point. These powers, or critical exponents, have universal values that only depend on a small number of *global* properties of the system under consideration. For example, binary mixtures, simple fluids, and uniaxial ferromagnets all exhibit the same set of critical exponents as the three-dimensional Ising model. However, the corresponding power-law behavior is only observed asymptotically close to the critical point, whereas at temperatures farther away from T_c (but still relatively close to it) one may observe classical or mean-field-like critical behavior. This *crossover* can be explained in terms of competing fixed points of a renormalization-group transformation and is in principle well understood. However, unlike the critical exponents, for which accurate results have been obtained from series expansions, renormalization-group calculations, experiments, and numerical calculations, the precise nature of the crossover from one universality class to another is still a point of discussion. In particular, it is an unsettled question to what extent this crossover is universal. There exist several field-theoretic calculations, but it has not yet been possible to verify their correctness by means of experiments. Measurements in the critical region are not only difficult, one also has to take great care to make the temperature distance to the critical point not too large, since one then would leave the critical region. As stated by the Ginzburg criterion, the crossover is a function of t/G, where $t = (T - T_c)/T_c$ is the reduced temperature and G a

system-dependent parameter. Throughout the crossover region, t has to be kept small, but t/G has to be varied over several decades. The large extent of the crossover region also emphasizes its experimental relevance: many measurements of critical exponents are actually made within this region rather than asymptotically close to the critical point and hence a detailed knowledge of crossover functions is required for a proper interpretation of the data. Since the Ginzburg parameter G is a function of the interaction range, it is well possible to construct such crossover functions from data obtained by means of simulations of systems with different interaction ranges, where for each system t is varied over a limited range only. In view of the large coordination numbers [$\mathcal{O}(10^4)$] that have to be reached within this approach, this is only feasible with an advanced algorithm.

We concentrate here on one specific crossover function, namely that for the susceptibility in a two-dimensional (2D) system, both below and above the critical temperature (see Refs. [21,22] for a more detailed discussion of this topic). In the 2D Ising model, the susceptibility χ diverges for $t \uparrow 0$ as $A_{\mathrm{I}}^{-}(-t)^{-7/4}$ and for $t \downarrow 0$ as $A_{\mathrm{I}}^{+}t^{-7/4}$, where the amplitudes $A_{\mathrm{I}}^{\pm}$ are known exactly. Mean-field theory, on the other hand, predicts a susceptibility that for $t \uparrow 0$ diverges as $1/(-2t)$ and for $t \downarrow 0$ as $1/t$. It is our aim to numerically determine the effective susceptibility exponent $\gamma_{\mathrm{eff}}^{\pm} = -d\ln\chi/d\ln t$, which is expected to interpolate smoothly between $7/4$ and 1. We have carried out MC simulations for square lattices with a maximum linear size $L = 1000$ and interaction ranges up to $R_m^2 = 10000$ (coordination number $z =$

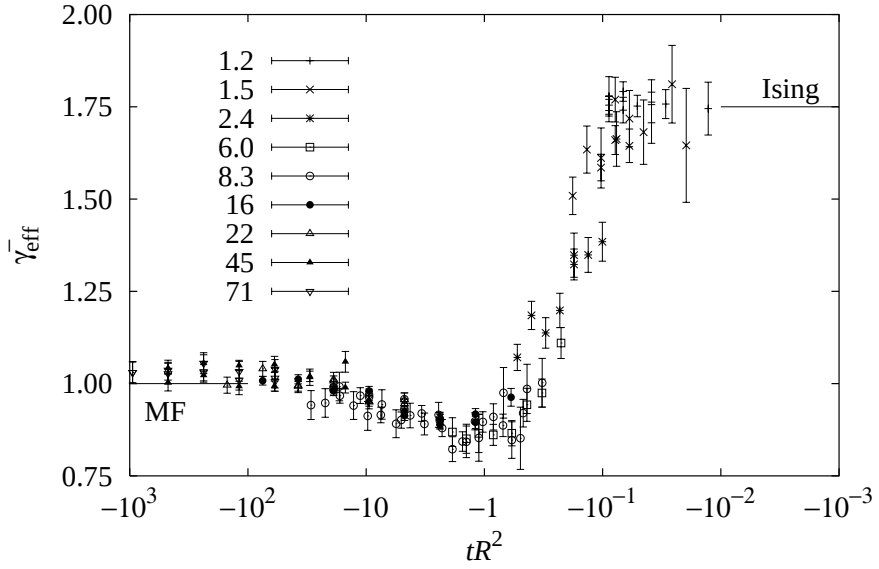

Fig. 2. The effective susceptibility exponent $\gamma_{\mathrm{eff}}^{-}$ for $T < T_{\mathrm{c}}$ as a function of the crossover variable tR^2.

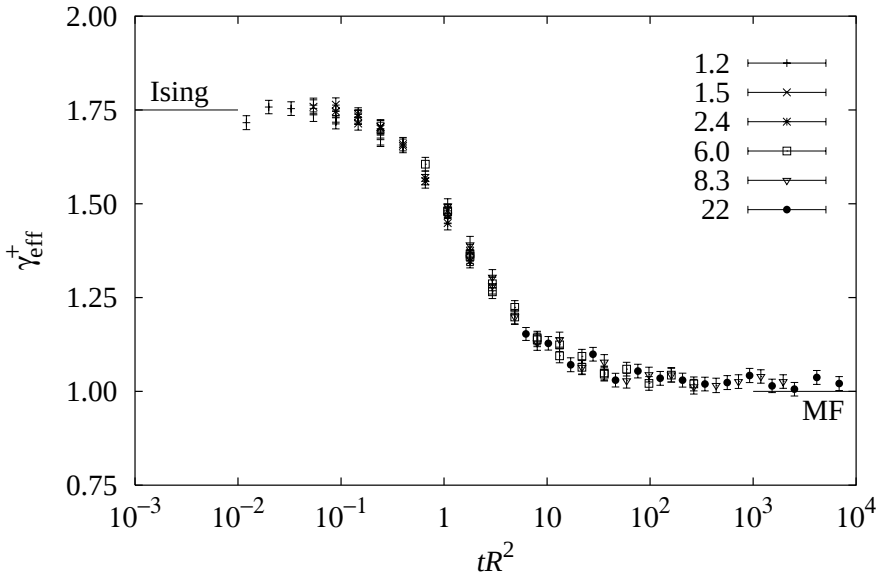

Fig. 3. The effective susceptibility exponent $\gamma^+_{\rm eff}$ for $T > T_{\rm c}$ as a function of the crossover variable tR^2.

31416). It has been shown that the Ginzburg parameter $G \propto R^{-2}$, where the effective interaction range $R^2 = z^{-1} \sum_{j \neq i} |\mathbf{r}_i - \mathbf{r}_j|^2$ ($|\mathbf{r}_i - \mathbf{r}_j| \leq R_m$) has been introduced to avoid lattice effects. For $t < 0$ the susceptibility is calculated from the fluctuation relation $\chi' = L^d(\langle m^2 \rangle - \langle |m| \rangle^2)/k_{\rm B}T$, whereas $\chi = L^d \langle m^2 \rangle / k_{\rm B}T$ was used for $t > 0$. The exponent $\gamma^{\pm}_{\rm eff}$ is obtained by numerical differentiation and shown as a function of t/G in Figs. 2 and 3, respectively.

Several observations can be made concerning these graphs. In the first place, one notices that both functions smoothly interpolate between the Ising exponent and its classical counterpart. Also the expectation that the crossover takes several decades in the parameter t/G is confirmed. However, there is a striking difference between $\gamma^-_{\rm eff}$ and $\gamma^+_{\rm eff}$: whereas the latter exhibits a gradual decrease from 7/4 to 1 when the distance to the critical point is increased, the former drops much more rapidly and even goes through a minimum where $\gamma_{\rm eff} < 1$, before reaching its asymptotic value. Interestingly, the occurrence of such a nonmonotonic variation has been inferred from RG calculations for three-dimensional systems. The results presented here are the first to show that, at least in the low-temperature regime, this behavior can actually be observed in systems as simple as the two-dimensional Ising model with an extended interaction range.

The fact that the curves in Figs. 2 and 3 overlap for different values of R suggests that the crossover functions possess a certain degree of universality. However, to what extent one may expect such universality in a region

where the correlation length no longer diverges is still an unanswered question. It has been suggested [23] that an additional length scale comes into play here. In order to investigate this possibility, we have carried out simulations of two-dimensional models that are very similar to those studied above, except that the interaction profile has been modified [24]. Instead of a constant interaction strength (block-shaped profile), a double-blocked potential was used, where each spin interacts with a strength K_1 with its z_1 neighbors within a distance $r \leq R_1$ (domain D_1) and with a strength K_2 with its z_2 neighbors within a distance $R_1 < r \leq R_2$ (domain D_2). In order to create a strong asymmetry, a strength ratio $\alpha = K_1/K_2 = 16$ was chosen. The outer interaction range was kept fixed at $R_2 = \sqrt{140}$, whereas the parameter R_1 was varied. This allowed us to realize two additional, qualitatively different situations: both $R_1 = \sqrt{4}$ and $R_1 = \sqrt{93}$ lead to an effective interaction range $R \approx \sqrt{50}$ [the previous definition for R is now generalized to $R^2 = (\alpha \sum_{i \in D_1} r_i^2 + \sum_{i \in D_2} r_i^2)/(\alpha z_1 + z_2)$] , but in the former case the inner domain contains only 12 out of 436 interaction neighbors, compared to 292 out of 436 in the latter case. This means that the integrated coupling ratio $\alpha z_1/z_2$, which indicates the relative contribution of the two domains to the total integrated coupling, is 0.45 in the first case and 32 in the second case. Extensive Monte Carlo simulations have been carried out for these and several other double-blocked interaction profiles. After a determination of the critical properties, we have calculated the crossover curve for the susceptibility in the region $t < 0$ for each of these profiles, in order to see whether the nonmonotonicity in Fig. 2 is a peculiarity of the equivalent-neighbor model. The critical temperature, normalized by the critical temperature of the mean-field model, indeed displays a clear nonuniversality: for $R_1^2 = 93$ the critical fluctuations turn out to be stronger suppressed than for $R_1^2 = 4$, even though the effective interaction range is almost identical. The data for the susceptibility are shown in Fig. 4. Since the critical amplitude of the susceptibility varies as $R^{-3/2}$, a data collapse is obtained for χ'/R^2. One observes how all data perfectly coincide with the crossover curve for the equivalent-neighbor model. The deviations from the curve at the right-hand side of the graph are caused by the fact that, sufficiently close to T_c, the diverging correlation length is truncated by the finite system size. For the systems with $R_1^2 = 4$ and $R_1^2 = 93$ (both with $R_2^2 = 140$) this happens in the figure at different temperatures, despite the fact that they have very similar values for the effective range R. The reason for this is that the data points pertain to different system sizes, viz. $L = 1000$ and $L = 300$, respectively. The inset shows that for the *same* system size ($L = 300$) the data points for both systems virtually coincide, even in the finite-size regime. The crossover function for the connected susceptibility appears to be insensitive to the introduction of an additional length scale in the interaction profile. We hence view this graph as a strong indication that crossover functions possess a considerable degree of universality.

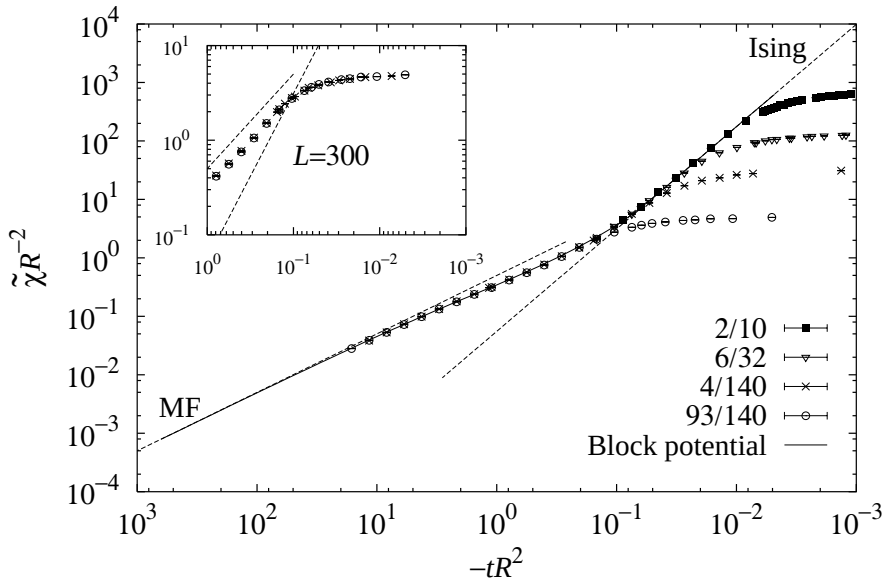

Fig. 4. The crossover function for the connected susceptibility below T_c, for the two-dimensional Ising model with a double-blocked interaction profile. $\tilde{\chi} = \chi'/C(R)$, where $C(R)$ is a range-dependent correction factor that accounts for the fact that the critical amplitude for small R deviates from the asymptotic range dependence. This only introduces a shift along the vertical axis. The solid curve indicates the crossover function for the block-shaped interaction profile and the dashed lines mark the mean-field ("MF") and the Ising asymptote. The numbers in the key refer to the values for R_1^2 and R_2^2 for each interaction profile.

4 Outlook and Conclusion

We have discussed a cluster algorithm for spin models with long-range interactions that is several orders of magnitude more efficient than conventional algorithms. Its usefulness has been demonstrated for a system with power-law interactions as well as for systems with medium-range interactions. In both cases, physical results have been obtained that until now could not be generated within a reasonable amount of computing time. However, the scope of the algorithm goes far beyond what could be presented here. As far as purely ferromagnetic interactions are concerned, it can be efficiently applied to any interaction profile, including anisotropic ones. Also the order parameter must not necessarily be Ising-like: the extension to general O(n) models [1] is similar to that for the original Wolff algorithm and the first application to a Potts model has already been published [25].

The generalization to a situation in which additional antiferromagnetic interactions are present is, in principle, also possible. Whereas competing interactions will move the system away from the percolation threshold (and

thus critical slowing down will no longer be optimally suppressed), one still has the advantage that not every individual spin has to be considered for inclusion in the cluster. Finally, it would be interesting to see whether this algorithm can be useful in other fields of physics where cluster algorithms have come to flourish.

Acknowledgements

I wish to thank Henk Blöte and Kurt Binder for the fruitful collaboration that has led to the work presented in this paper. I am grateful to Holger Meßingfeld for producing the data shown in Fig. 1 and performing the least-squares fits for the inverse-square chain.

References

1. E. Luijten and H. W. J. Blöte, Int. J. Mod. Phys. C **6**, 359 (1995).
2. R. H. Swendsen and J.-S. Wang, Phys. Rev. Lett. **58**, 86 (1987).
3. U. Wolff, Phys. Rev. Lett. **62**, 361 (1989).
4. P. W. Kasteleyn and C. M. Fortuin, J. Phys. Soc. Jpn. Suppl. **26s**, 11 (1969).
5. C. M. Fortuin and P. W. Kasteleyn, Physica **57**, 536 (1972).
6. E. Luijten and H. W. J. Blöte, Phys. Rev. B **56**, 8945 (1997).
7. E. Luijten and H. Meßingfeld, in preparation.
8. J. F. Nagle and J. C. Bonner, J. Phys. C **3**, 352 (1970).
9. P. W. Anderson and G. Yuval, J. Phys. C **4**, 607 (1971).
10. B. G. S. Doman, Phys. Stat. Sol. (b) **103**, K169 (1981).
11. G. V. Matvienko, Theor. Math. Phys. **63**, 635 (1985).
12. J. O. Vigfusson, Phys. Rev. B **34**, 3466 (1986).
13. M. Aizenman, J. T. Chayes, L. Chayes, and C. M. Newman, J. Stat. Phys. **50**, 1 (1988).
14. J. L. Monroe, R. Lucente, and J. P. Hourlland, J. Phys. A **23**, 2555 (1990).
15. M. J. Wragg and G. A. Gehring, J. Phys. A **23**, 2157 (1990).
16. R. Manieri, Phys. Rev. A **45**, 3580 (1992).
17. Z. Glumac and K. Uzelac, J. Phys. A **26**, 5267 (1993).
18. J. L. Monroe, J. Stat. Phys. **76**, 1505 (1994).
19. S. A. Cannas and A. C. N. de Magalhães, J. Phys. A **30**, 3345 (1997).
20. E. Luijten, Phys. Rev. E, to be published (see also cond-mat/9811332).
21. E. Luijten, H. W. J. Blöte, and K. Binder, Phys. Rev. Lett. **79**, 561 (1997).
22. E. Luijten, H. W. J. Blöte, and K. Binder, Phys. Rev. E **56**, 6540 (1997).
23. M. A. Anisimov, A. A. Povodyrev, V. D. Kulikov, and J. V. Sengers, Phys. Rev. Lett. **75**, 3146 (1995).
24. E. Luijten and K. Binder, in preparation.
25. Z. Glumac and K. Uzelac, Phys. Rev. E **58**, 4372 (1998).